

EFFECT OF SURFACE FRICTION ON THE STRUCTURE OF BAROTROPICALLY UNSTABLE TROPICAL DISTURBANCES

R. T. WILLIAMS

Naval Postgraduate School, Monterey, Calif.

T. K. SCHMINKE¹

University of Utah, Salt Lake City, Utah

R. L. NEWMAN²

Naval Postgraduate School, Monterey, Calif.

ABSTRACT

The structure of barotropically unstable disturbances in the Tropics is studied with a two-level quasi-geostrophic model. An Ekman layer is attached to the lower boundary. The equations are linearized and the most unstable mode is found numerically by using the initial value technique. Computations are made for a shear-zone wind profile and a jet profile; these fields are independent of height. The disturbance structure is found to be critically dependent on the absolute vorticity gradient in the mean flow. The predicted disturbance structures contain a number of features that are observed in tropical wave disturbances.

1. INTRODUCTION

Synoptic scale disturbances in the tropical atmosphere have long been recognized (Palmer 1951, Riehl 1954). We are concerned with the wave disturbances that occur in the lower troposphere [following La Seur (1963), we make no distinction between easterly waves and equatorial waves]. In the lower troposphere these disturbances have a "cold core" structure; that is, the rising air is somewhat cooler than the sinking air (Starr and Wallace 1964). Zipser (1969) has pointed out that this cold core may be the result of downdrafts in the convective regions. Chang et al. (1970) and Nitta (1970) found warm core structures at higher levels with significant correlations between temperature and vertical velocity. Vertical motions associated with these waves are generally upward east of the wave axis and downward to the west (Yanai and Nitta 1967).

The energy source for these waves is not known. Baroclinic instability is unlikely because of the smallness of the Coriolis parameter. Yanai (1961) and Charney (1963) have suggested that easterly waves arise from barotropic instability. This is consistent with Charney's (1963) scale analysis which indicates that, in the absence of condensation, large-scale motions in the Tropics are governed by the barotropic vorticity equation. Also, the spectral analyses of Wallace and Chang (1969) show disturbance tilts with latitude which are opposite to the horizontal wind shear. This indicates a conversion of kinetic energy from the mean flow to the disturbance.

A third possible energy source for the tropical wave disturbances is latent heat of condensation. This mechanism is consistent with observations of warm core structures at upper levels (Chang et al. 1970). Yamasaki (1969) studied the influence of Conditional Instability of the Second Kind (CISK) (Ooyama 1969, Charney and Eliassen 1964, Kuo 1965) on linearized disturbances in an atmosphere with vertical shear. His solutions display many features that are observed in actual tropical wave disturbances. Holton (1971) has obtained similar results with a model that contains a moving heat source in an atmosphere with vertical wind shear. Manabe et al. (1970) observed similar disturbances in their general circulation experiment. These studies strongly suggest that many tropical disturbances are driven by latent heat of condensation. However, the CISK mechanism cannot operate until a pre-existing disturbance has organized the convective elements. This disturbance could arise from barotropic instability as has been demonstrated by Bates (1970) with a numerical model. In this paper, we will determine the structure of barotropically unstable disturbances that include surface friction. Disturbances that are driven by CISK and that arise from barotropic instability should have some features of barotropically unstable disturbances.

Kuo (1949) examined the stability characteristics of a barotropic zonal current and found that instability is possible only if the gradient of the absolute vorticity changes sign somewhere in the region. Nitta and Yanai (1969) report that this criteria is satisfied at certain times of the year in the tropical Pacific. They also computed growth rates and wave structures based on the observed mean winds. Lipps (1970) has studied barotropic instability in the Tropics with a simplified wind profile.

¹ Present affiliation: Air Force Global Weather Central, Offutt Air Force Base, Nebr.

² Present affiliation: U.S. Navy Fleet Weather Facility, London, England.

In this paper, idealized mean wind profiles are used that approximately represent tropical flows, and baroclinic effects are excluded by making the mean wind independent of height. The quasi-geostrophic prediction equations are used in this study and they should accurately depict the barotropic instability process. Certain features of the solutions will be in error near the Equator, but Matsuno (1966) has shown with a barotropic model that quasi-geostrophic motions are identifiable near the Equator provided the wavelength is not too long. In another study with a baroclinic model, Yamasaki (1969) has found that the quasi-geostrophic error is small at 20 deg. lat.

To obtain the weather patterns, it is important to determine the vertical motion field associated with a growing wave. Jacobs and Wiin-Nielsen (1966) have shown that the most unstable mode in a stratified barotropic current is the mode that is independent of height and that contains no vertical motion. Thus a mechanism is needed in the solutions that will initiate vertical motions. This can be accomplished by the addition of a surface friction layer. Hurricane models (Charney and Eliassen 1964, Kuo 1965, Ooyama 1969) have shown the importance of frictionally induced vertical motions in the Tropics.

The quasi-geostrophic equations are simplified through the introduction of a two-level model. Bates (1970) also used a two-level quasi-geostrophic model. The equations are linearized and solved numerically by the initial value technique. Growth rates and wave structures are computed for two basic wind profiles, and the wave structures obtained are compared with observed features of tropical wave disturbances.

2. BASIC EQUATIONS

The quasi-geostrophic vorticity equation in pressure coordinates is

$$\frac{\partial}{\partial t} \nabla^2 \Psi + \mathbf{k} \times \nabla \Psi \cdot \nabla \nabla^2 \Psi + \beta_0 \frac{\partial \Psi}{\partial x} - f_0 \frac{\partial \omega}{\partial p} = 0 \quad (1)$$

where $f_0 = 2\Omega \sin \varphi_0$, $\beta = 2\Omega \cos \varphi_0/a$, $\omega = dp/dt$, $\Psi =$ stream function, φ_0 is the central reference latitude, and a is the radius of the earth. When $\omega = 0$ this equation reduces to the barotropic vorticity equation, which indicates that barotropic instability should be properly described by this model. The quasi-geostrophic first law of thermodynamics is

$$\frac{\partial}{\partial t} \frac{\partial \Psi}{\partial p} + \mathbf{k} \times \nabla \Psi \cdot \nabla \frac{\partial \Psi}{\partial p} + \frac{\sigma \omega}{f_0} = 0 \quad (2)$$

where

$$\sigma = \frac{R^2 T_s}{p^2 g} \left(\frac{dT_s}{dz} + \frac{g}{c_p} \right).$$

The quantity T_s is obtained from a standard atmosphere. The quasi-geostrophic relation $\Psi = gz/f_0$ is used in deriving eq (2).

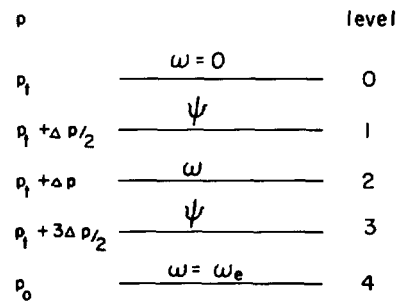


FIGURE 1.—Schematic diagram of the vertical modeling.

A simple two-level model is constructed by dividing the atmosphere between $p = p_i$ and $p = p_0$ into four layers of pressure differential $\Delta p/2$. Here p_0 is the sea-level pressure and p_i is the pressure at the top of the easterly wave regime. The levels between the layers are numbered from 0 to 4 and the variables are arranged as shown in figure 1. The boundary condition at $p = p_i$ is $\omega_0 = 0$, which prohibits vertical energy propagation. Charney (1969) has shown that an appreciable vertical energy propagation is unlikely for these waves. At $p = p_0$ the boundary condition is $\omega_4 = \omega_e$ where ω_e is the frictionally induced ω at the top of the Ekman layer. Charney and Eliassen (1949) derived the following expression for ω_e :

$$\omega_e = -\rho_0 g \left(\frac{A_e}{2f_0} \right)^{1/2} \sin 2\alpha (\zeta_g)_4 \quad (3)$$

where A_e is the eddy viscosity, α is the surface inflow angle, and ζ_g is the geostrophic vorticity. Holton et al. (1971) have shown that this expression is good in the Tropics down to a latitude of a few degrees. These results were obtained for a small amplitude neutral traveling wave. The last variable in eq (3) is approximated by

$$(\zeta_g)_4 \cong (\zeta_g)_3 = \nabla^2 \Psi_3. \quad (4)$$

We apply the vorticity equation [eq (1)] at levels 1 and 3 and introduce finite differences in p , arriving at

$$\frac{\partial}{\partial t} \nabla^2 \Psi_1 + \mathbf{k} \times \nabla \Psi_1 \cdot \nabla \nabla^2 \Psi_1 + \beta_0 \frac{\partial \Psi_1}{\partial x} - \frac{f_0 \omega_2}{\Delta p} = 0 \quad (5)$$

and

$$\frac{\partial}{\partial t} \nabla^2 \Psi_3 + \mathbf{k} \times \nabla \Psi_3 \cdot \nabla \nabla^2 \Psi_3 + \beta_0 \frac{\partial \Psi_3}{\partial x} - \frac{f_0 (\omega_e - \omega_2)}{\Delta p} = 0. \quad (6)$$

The first law of thermodynamics eq (2) is applied at level 2:

$$\frac{\partial}{\partial t} (\Psi_1 - \Psi_3) + \mathbf{k} \times \nabla \frac{(\Psi_1 + \Psi_3)}{2} \cdot \nabla (\Psi_1 - \Psi_3) - \frac{\Delta p \sigma_2 \omega_2}{f_0} = 0. \quad (7)$$

We now define the following quantities

$$\Psi_M = (\Psi_1 + \Psi_3)/2, \quad \Psi_T = (\Psi_1 - \Psi_3)/2, \quad (8)$$

which imply that

$$\Psi_1 = \Psi_M + \Psi_T, \quad \Psi_3 = \Psi_M - \Psi_T. \quad (9)$$

Here Ψ_T is proportional to the layer thickness, hence it is proportional to the mean temperature of the layer.

If we add eq (5) and (6), divide by 2, and use the definitions (eq 8) we obtain

$$\frac{\partial}{\partial t} \nabla^2 \Psi_M + \mathbf{k} \times \nabla \Psi_M \cdot \nabla \nabla^2 \Psi_M + \mathbf{k} \times \nabla \Psi_T \cdot \nabla \nabla^2 \Psi_T + \beta_0 \frac{\partial \Psi_M}{\partial x} - \frac{f_0 \omega_e}{2 \Delta p} = 0. \quad (10)$$

The second forecast equation is obtained by subtracting eq (6) from (5) and by eliminating ω_2 with eq (7):

$$\frac{\partial}{\partial t} (\nabla^2 - \mu^2) \Psi_T + \mathbf{k} \times \nabla \Psi_M \cdot \nabla (\nabla^2 - \mu^2) \Psi_T + \mathbf{k} \times \nabla \Psi_T \cdot \nabla \nabla^2 \Psi_M + \beta_0 \frac{\partial \Psi_T}{\partial x} + \frac{f_0 \omega_e}{2 \Delta p} = 0 \quad (11)$$

where

$$\mu^2 = 2f_0^2 / \Delta p^2 \sigma_2.$$

We now linearize and nondimensionalize the forecast equations. The independent variables are nondimensionalized as follows: $x = Lx'$, $y = Ly'$, and $t = L/Ut'$. The stream function is written

$$\Psi_M = -LU \int \bar{u}(y') dy' + \psi_M(x', y', t') \quad (12)$$

and

$$\Psi_T = \psi_T(x', y', t').$$

The quantities ψ_M and ψ_T are very small and the mean current \bar{u} is a function of y' only. Introduce the nondimensional quantities into eq (10) and (11) and linearize by dropping the small quantities. If we drop the primes and use eq (3), the final equations can be written

$$\left(\frac{\partial}{\partial t} + \bar{u} \frac{\partial}{\partial x} \right) \nabla^2 \psi_M + \left(\hat{\beta} - \frac{d^2 \bar{u}}{dy^2} \right) \frac{\partial \psi_M}{\partial x} + \gamma \nabla^2 (\psi_M - \psi_T) = 0 \quad (13)$$

$$\left(\frac{\partial}{\partial t} + \bar{u} \frac{\partial}{\partial x} \right) (\nabla^2 - \epsilon) \psi_T + \left(\hat{\beta} - \frac{d^2 \bar{u}}{dy^2} \right) \frac{\partial \psi_T}{\partial x} - \gamma \nabla^2 (\psi_M - \psi_T) = 0 \quad (14)$$

where

$$\epsilon = L^2 \mu^2, \quad \hat{\beta} = \beta_0 L^2 U^{-1}, \quad \gamma = \frac{1}{U/f_0 L} \frac{\sin 2\alpha}{2 \Delta p / \rho_4 g} \left(\frac{A_e}{2f_0} \right)^{1/2}$$

Consistent with the assumption that \bar{u} is constant in time, we have neglected $\partial \bar{u} / \partial y$ in the frictional terms. The quantity γ is the ratio of the square root of the Ekman number (Greenspan 1968) to the Rossby number.

Equations (13) and (14) indicate that, in the absence of friction, the ψ_M and ψ_T fields will evolve independently. Jacobs and Wiin-Nielsen (1966) have shown that in the frictionless case the ψ_M mode has a larger maximum growth rate than the ψ_T mode. Since the vertical motion field associated with the ψ_M mode is zero, it is clearly necessary to tie the ψ_M and ψ_T fields together with friction in order to obtain a vertical motion field.

We shall bound the motion in y by placing rigid walls of $y = \pm W$. The boundary conditions then become

$$\psi_M(x, W, t) = \psi_M(x, -W, t) = \psi_T(x, W, t) = \psi_T(x, -W, t) = 0. \quad (15)$$

The linear equations (13) and (14) can be solved with the use of these boundary conditions.

3. SOLUTION PROCEDURE

Equations (13) and (14) can be Fourier transformed in x since all quantities are periodic in x . The resulting equations can be solved either with the normal mode method or with the initial value method. The normal mode method gives the phase speeds, growth rates, and wave structures for all modes, while the initial value approach gives the phase speed, growth rate, and wave structure of only the most unstable mode. We will use the initial value method because we only require information about the most unstable mode since it is the most likely to be observed in nature.

It is convenient to write ψ_M and ψ_T in the following form:

$$\psi_M = A(y, t) \cos kx + B(y, t) \sin kx \quad (16)$$

and

$$\psi_T = C(y, t) \cos kx + D(y, t) \sin kx$$

where k is the x -wave number. Substitute eq (16) into eq (13) and separately equate to zero the coefficients of $\cos kx$ and $\sin kx$. The $\cos kx$ terms give

$$\left(\frac{\partial^2}{\partial y^2} - k^2 \right) \frac{\partial A}{\partial t} = -k \left[\bar{u} \left(\frac{\partial^2}{\partial y^2} - k^2 \right) + \left(\hat{\beta} - \frac{d^2 \bar{u}}{dy^2} \right) \right] B - \gamma \left(\frac{\partial^2}{\partial y^2} - k^2 \right) (A - C) \quad (17)$$

and the $\sin kx$ terms give

$$\left(\frac{\partial^2}{\partial y^2} - k^2 \right) \frac{\partial B}{\partial t} = k \left[\bar{u} \left(\frac{\partial^2}{\partial y^2} - k^2 \right) + \left(\hat{\beta} - \frac{d^2 \bar{u}}{dy^2} \right) \right] A - \gamma \left(\frac{\partial^2}{\partial y^2} - k^2 \right) (B - D). \quad (18)$$

The same procedure applied to eq (14) gives for the $\cos kx$ terms

$$\left[\frac{\partial^2}{\partial y^2} - (k^2 + \epsilon) \right] \frac{\partial C}{\partial t} = -k \left[\bar{u} \left(\frac{\partial^2}{\partial y^2} - (k^2 + \epsilon) \right) + \left(\hat{\beta} - \frac{d^2 \bar{u}}{dy^2} \right) \right] D + \gamma \left(\frac{\partial^2}{\partial y^2} - k^2 \right) (A - C) \quad (19)$$

and for the $\sin kx$ terms

$$\left[\frac{\partial^2}{\partial y^2} - (k^2 + \epsilon) \right] \frac{\partial D}{\partial t} = k \left[\bar{u} \left(\frac{\partial^2}{\partial y^2} - (k^2 + \epsilon) \right) + \left(\hat{\beta} - \frac{d^2 \bar{u}}{dy^2} \right) \right] C + \gamma \left(\frac{\partial^2}{\partial y^2} - k^2 \right) (B - D). \quad (20)$$

Equations (17)–(20) are solved numerically by introducing finite differences in y and t . The second derivative with respect to y of a typical variable A is approximated as

$$\left(\frac{\partial^2 A}{\partial y^2}\right)_j = \frac{(A_{j+1} - 2A_j + A_{j-1}))}{\Delta y^2} \quad (21)$$

where j is the grid index and Δy is the distance between grid points. Centered time-differences are used for all quantities except those involving friction; the frictional terms are evaluated at the previous time step. The integration begins with a forward time step.

The boundary conditions (eq 15) become

$$A=B=C=D=0 \text{ at } y = \pm W.$$

The second-order equations for the time tendencies are solved by the exact method of Richtmyer (1967, p. 101).

Equations (17)–(20) can be solved numerically as a function of ϵ , $\hat{\beta}$, γ , and $\bar{u}(y)$ for any initial conditions. Equations (13) and (14) will, in general, have a set of discrete normal mode solutions as well as a continuous spectrum of solutions (Case 1960, Pedlosky 1964, Yanai and Nitta 1968). Only the normal mode solution can give appreciable growth and after a sufficient period of time the most unstable mode will predominate.

In all results to be presented, the initial fields of A and B are random in y and C and D are zero. The integration is continued until the growth is clearly exponential. The growth rate, phase speed, and wave structure of the most unstable mode are then extracted.

4. RESULTS

In this paper, we examine a shear zone wind profile and a jet wind profile. Charney (1963) suggested that, when the intertropical convergence zone is shifted away from the Equator, a shear zone could be formed by the transport of angular momentum from different regions. To represent the resulting profile, we choose

$$\bar{u} = -\tanh y, \quad (22)$$

which is shown in figure 2. Lipps (1970) has used this wind profile in an inviscid study of barotropic instability in the Tropics. This wind field is antisymmetric with respect to the intertropical convergence zone, located at $y=0$. A jet wind profile which is symmetric about $y=0$ is given by

$$\bar{u} = \text{sech}^2 y. \quad (23)$$

This jet profile is shown in figure 3. The U and the L which appear in the scale analysis can now be interpreted as the maximum \bar{u} and the y scale of \bar{u} , respectively. We note that a constant velocity can be added to the expressions for \bar{u} without changing the growth rate of the disturbance or its structure. The added constant could be chosen, for example, to make \bar{u} everywhere negative. If

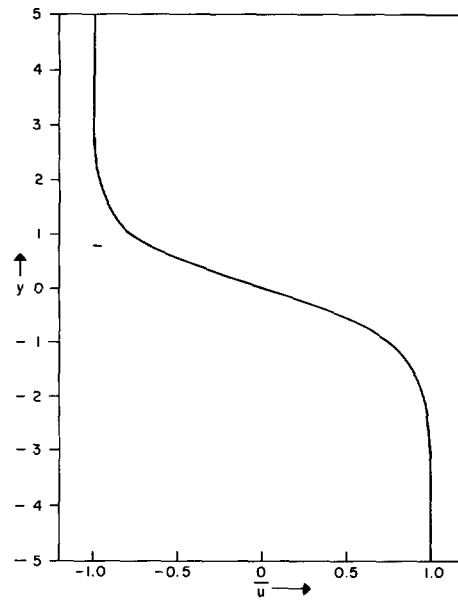


FIGURE 2.—Mean wind profile $\bar{u} = -\tanh y$.

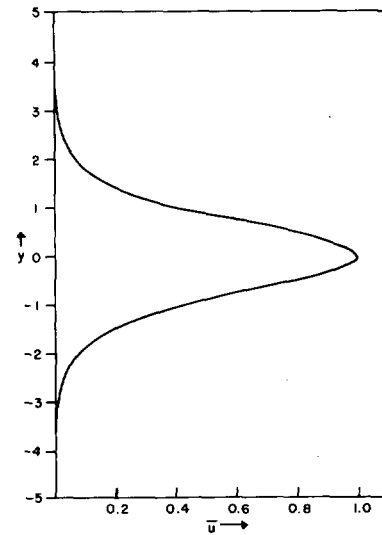


FIGURE 3.—Mean wind profile $\bar{u} = \text{sech}^2 y$.

this were done with the jet profile (eq 23), the minimum easterly speed would occur in the intertropical convergence zone at $y=0$. If this profile were reversed, it could represent an easterly jet. The phase relations in our solutions can be reversed to match this profile if $\hat{\beta} = 0$.

All numerical integrations are performed with the non-dimensional constants

$$\Delta y = 1/8, \quad \Delta t = 0.09, \quad \text{and } W = 5.$$

The various experiments are given in table 1 as a function of \bar{u} , k , $\hat{\beta}$, γ , and ϵ . The growth rate n and the phase speed c_r are also given. For each set of the quantities $\bar{u}(y)$, $\hat{\beta}$, γ , and ϵ , a series of calculations was made to determine the growth rate as a function of k . The value of k that corresponds to the maximum growth rate is given in the table.

TABLE 1.—Compilation of numerical experiments

Experiment	\bar{u}	k	$\hat{\beta}$	γ	ϵ	n	c_r
1	$-\tanh y$	0.45	0	0		0.165	0
2	$-\tanh y$	0.45	0	0.014	0.10	0.153	0
3	$-\tanh y$	0.6	0.368	0.028	0.40	0.069	-0.42
4	$\text{sech}^2 y$	0.9	0	0.014	0.10	0.139	0.454
5	$\text{sech}^2 y$	1.3	0.368	0.028	0.40	0.050	0.422

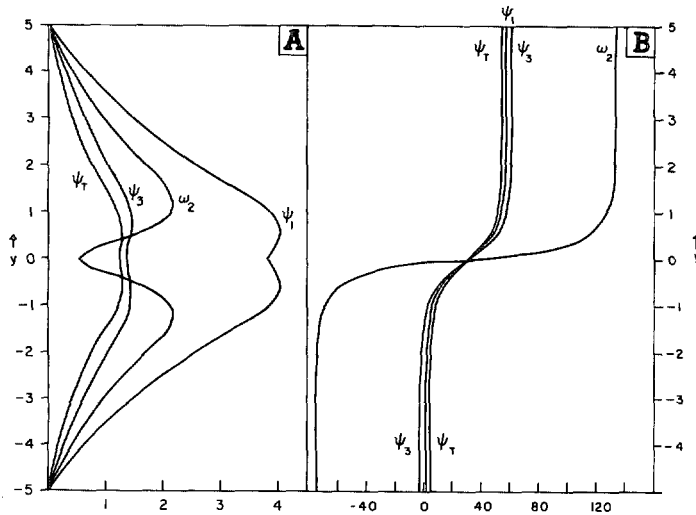


FIGURE 4.—(A) amplitudes of ψ_1 , ψ_3 , ψ_T , and ω_2 for experiment 2. The quantities ψ_1 , ψ_3 , and ψ_T have the same scale; ω_2 is given on a different scale. (B) phases of ψ_1 , ψ_3 , ψ_T , and ω_2 for experiment 2 in deg. Each dependent variable is expressed in the form $P \cos(kx - \delta)$, where P is the amplitude and δ is the phase angle.

As previously mentioned, Kuo (1949) has shown that a barotropic zonal current can be unstable only if the gradient of the absolute vorticity changes sign. In our notation this condition becomes

$$(d^2\bar{u}/dy^2)_{max} > \hat{\beta}. \tag{24}$$

This condition also holds for stratified flow when \bar{u} is independent of height.

Garcia (1956) found that the shear zone profile (eq 22) is barotropically unstable when $0 < k < 1$. Betchov and Criminale (1967) computed the eigen solutions for this profile throughout this range and they found the maximum instability at $k = 0.45$. Experiment 1 is a check case with friction and the beta term excluded. The wave number of maximum instability agrees with the value obtained by Betchov and Criminale, but the growth rate ($n = 0.165$) is somewhat less than their value. This difference arises from the finite distance to the side boundaries and from the numerical approximations.

Friction is added in experiment 2 which is otherwise the

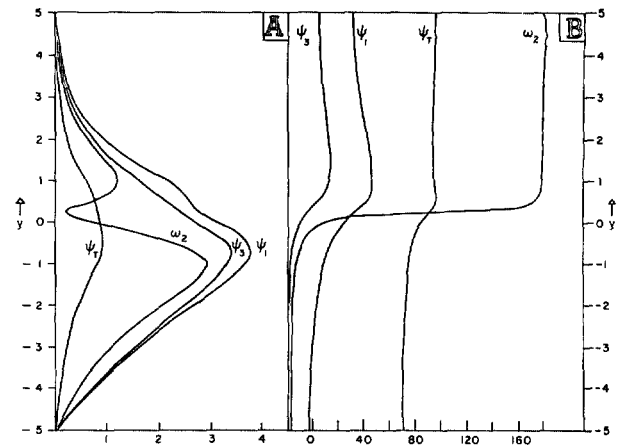


FIGURE 5.—(A) amplitudes of ψ_1 , ψ_3 , ψ_T , and ω_2 for experiment 3. (B) phases of ψ_1 , ψ_3 , ψ_T , and ω_2 for experiment 3 in deg.

same as experiment 1. In experiment 2, the growth rate is reduced by an amount that is of the order of the frictional parameter, γ . Figure 4A contains the amplitudes of ψ_1 , ψ_3 , ψ_T , and ω_2 for this experiment as functions of y . The units are arbitrary since the basic equations are linear. The ω_2 field is computed from eq (7) with the use of eq (8) and (16). All quantities show double maxima with the extremes occurring near the edges of the shear zone in \bar{u} . Although surface friction has a small effect on the growth rate, it has a large effect on the disturbance structure since ψ_3 is much smaller than ψ_1 . In the frictionless case, the most unstable mode has $\psi_1 = \psi_3$. Figure 4B contains the phase angles for ψ_1 , ψ_3 , ψ_T , and ω_2 for this experiment as functions of y . All quantities show a rapid phase increase that is opposite to the wind shear through the shear zone and the three ψ fields are nearly coincident. This solution does not exhibit the eastward tilt with height that is observed in some easterly waves. It is seen that the maximum rising motion at level 2 (ω_2 minimum) is everywhere upwind of the level 3 streamline trough axis (ψ_3 minimum) except at $y=0$. This corresponds to the unsettled weather that is often observed to the east of the trough axis in easterly waves. To the south of $y=0$ the rising motion is west of the trough axis. It is not known if this structure is observed for waves associated with a shear zone, but in this model it is an immediate consequence of the symmetry relations. The figure also shows a weak positive correlation between ω_2 and ψ_T . This indicates energy conversion from disturbance kinetic to disturbance potential energy.

Experiment 3 includes the beta effect and a doubled y -scale, L , of the mean flow. These parametric differences between experiments 2 and 3 are shown in table 1. In practice, the beta term is neglectable only if the y -scale is sufficiently small. If the same value of β (dimensional) were used in experiment 2 or in 3, it would turn out that the beta effect would be nearly neglectable in the former experiment. Thus our change in L between experiments 2 and 3

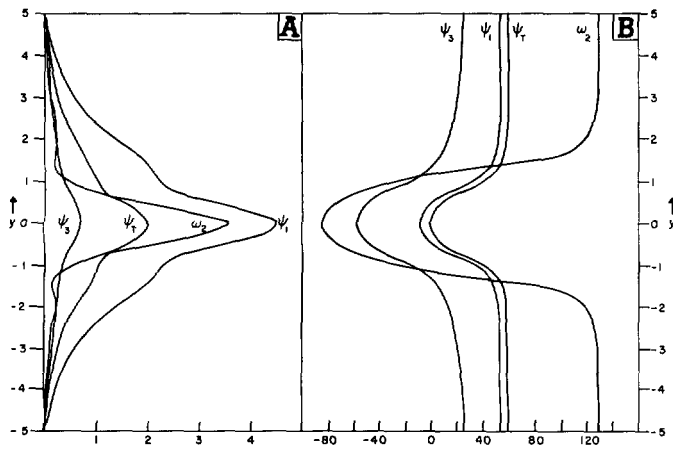


FIGURE 6.—(A) amplitudes of ψ_1 , ψ_3 , ψ_T , and ω_2 for experiment 4. (B) phases of ψ_1 , ψ_3 , ψ_T , and ω_2 for experiment 4 in deg.

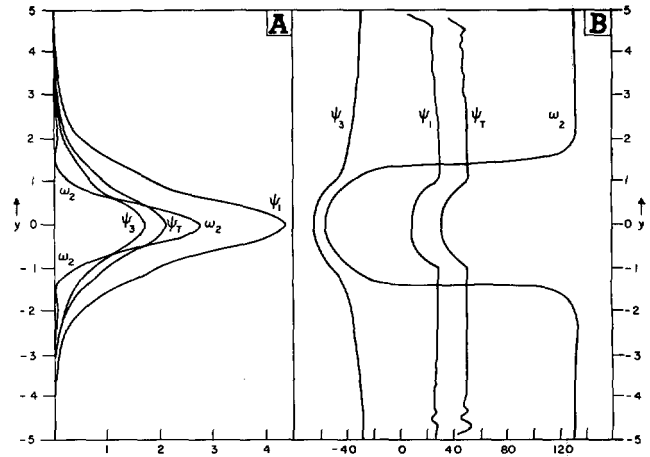


FIGURE 7.—(A) amplitudes of ψ_1 , ψ_3 , ψ_T , and ω_2 for experiment 5. (B) phases of ψ_1 , ψ_3 , ψ_T , and ω_2 for experiment 5 in deg.

simulates the actual beta effect on these waves. The stability criterion (eq 24) for the shear zone profile is

$$0.77 > \hat{\beta}.$$

With $\hat{\beta}=0.368$, the growth rate is reduced from 0.153 to 0.069. The wave number with the maximum growth rate is increased from 0.45 to 0.60. This is expected since the presence of beta tends to stabilize the longer waves. The presence of beta also leads to retrogression since the phase speed is reduced from 0 to -0.42 . The amplitudes of ψ_1 , ψ_3 , ψ_T , and ω_2 are given in figure 5A. The solutions are not symmetric about $y=0$ since the absolute vorticity gradient is not an odd function of y . In this experiment, the ψ_3 curve is much closer to the ψ_1 curve than was the case with experiment 2. The vertical motion is much larger below $y=0$ than it is above it. This corresponds to the precipitation pattern that was observed in the eastern Pacific by Sadler (1963). In this region, the intertropical convergence zone is shifted well north of the Equator and lies in a region of cyclonic wind shear. Thus the wind profile (eq 22) which is used in this experiment is appropriate for the region that was studied by Sadler. Figure 5B contains the phase angles for ψ_1 , ψ_3 , ψ_T , and ω_2 for experiment 3. The figure shows that the disturbance tilts eastward with height with an average phase difference between ψ_1 and ψ_3 of about 30 deg. North of the shear zone the streamline trough lies nearly in the center of the sinking region. South of the shear zone, where the vertical velocity is much larger, the streamline trough is found in the center of the rise region. This experiment was repeated with a different value of ϵ and the same patterns were obtained except for some quantitative changes.

Lipps (1962) has determined the barotropic stability properties of the jeb profile (eq 23) with friction neglected. He found for $\hat{\beta}=0$ that unstable waves exist in the range $0 < k < 2$. Growth rates computed by Betchov

and Criminale (1967) indicate a broad maximum around $k=0.9$. Our experiment 4, which includes surface friction, agrees with their results as can be seen in table 1. The growth rate is 0.139 and the phase speed is 0.454. The amplitudes of ψ_1 , ψ_3 , ψ_T , and ω_2 are shown in figure 6A. Each quantity has a distinct maximum at $y=0$ and ψ_1 is much larger than ψ_3 . Figure 6B contains the phase angles for ψ_1 , ψ_3 , ψ_T , and ω_2 for this experiment. The disturbance tilts eastward with height with the phase difference between ψ_1 and ψ_3 being about 40 deg. Outside the central jet zone, the rising motion is about 100 deg. to the east of the low-level trough position. However, this is of little synoptic importance since the vertical motions are small in this region. In the central region, where ω_2 is large, the rising motion is actually located to the west of the low-level trough axis.

Experiment 5 includes the beta effect and a doubled y -scale of the mean flow. The stability criterion (eq 24) for the jet profile is

$$2/3 > \hat{\beta}.$$

With $\hat{\beta}=0.368$, the growth rate is decreased from 0.139 to 0.050. The wave number with the maximum growth rate is increased from 0.9 to 1.3. The presence of beta causes a slight reduction in phase speed from 0.454 to 0.422. The amplitudes of ψ_1 , ψ_3 , ψ_T , and ω_2 are given in figure 7A. The solutions are symmetric about $y=0$ because the absolute vorticity gradient is an even function of y for both $\hat{\beta}=0$ and $\hat{\beta}\neq 0$. The curves are generally similar to those obtained in experiment 4 except that ψ_3 is a larger percentage of ψ_1 than it was in experiment 4. The phase angles for ψ_1 , ψ_3 , ψ_T , and ω_2 are given in figure 7B. The disturbance tilts eastward with height, the difference between ψ_1 and ψ_3 being about 60 deg. In the central region, where ω_2 is finite, the rising motion maximum lies just to the east of the low-level trough axis.

5. CONCLUSIONS

In this paper, numerically computed barotropically unstable disturbances are compared with tropospheric waves that occur in the tropical easterlies. A two-level quasi-geostrophic model is used with an attached Ekman layer. The most unstable solutions are obtained numerically by the initial value procedure. Two basic wind profiles are used: (1) a shear zone profile ($\bar{u} = -\tanh y$) and (2) a jet profile ($\bar{u} = \text{sech}^2 y$). The solution structures are computed for each profile with $\hat{\beta} = 0$ and $\hat{\beta} \neq 0$.

Observational studies indicate that certain tropical wave disturbances have the following main characteristics: (1) rising motion upwind of the wave trough and sinking motion downwind, (2) eastward tilt of the disturbance with height, and (3) a weak negative correlation at lower levels between vertical motion and temperature (Nitta 1970). These characteristics cannot be obtained with a pure barotropic model because of the absence of vertical motion. In our model, the most unstable disturbance contains vertical motion only when surface friction is present. Experiments 2 and 5 satisfy disturbance characteristic (1) and experiments 3, 4, and 5 satisfy characteristic (2). The latitudinal vertical motion pattern obtained from experiment 3 corresponds to precipitation patterns observed in the eastern Pacific (Sadler 1963). All the experiments that include friction satisfy characteristic (3) since they show a weak negative correlation between the vertical velocity and the temperature. This fact implies an energy conversion from disturbance kinetic to disturbance potential energy; such a conversion is an automatic consequence of the fact that the basic state contains no potential energy. In each experiment, the disturbance velocities are greater at the upper level because friction is applied at the lower level. However, in the more realistic experiments which include beta, the disturbance velocities at the two levels are closer in magnitude.

It is useful to examine the wavelengths and doubling times of the most unstable waves for typical values of the constants. The parametric values given in table 1 correspond to the following dimensional constants: $U = 10$ m/s, $\Delta p = 200$ mb, $\varphi_0 = 15$ deg., $dT_s/dz = 6.4^\circ\text{C}/\text{km}$, and $L = 200$ km (exp. 1, 2, and 4) or $L = 400$ km (exp. 3 and 5). This value of Δp restricts the disturbance to the lower 400 mb of the atmosphere. The wavelengths of the most unstable waves range from 1400 km for experiment 4 to 4180 km for experiment 3. The doubling times range from 0.98 days for experiment 1 to 6.45 days for experiment 5. These values are reasonable for observed tropical wave disturbances. The model predicts vertical velocities which are synoptically significant. For a disturbance with a maximum north-south velocity of 5 m/s and a wavelength of 2000 km, the maximum vertical velocity is about 1 cm/s.

Our experiments show that the disturbance structure is critically dependent on the absolute vorticity gradient in the mean current. Merritt (1964) has pointed out that waves in the easterlies do have a variable structure and our results suggest that this variation could arise from changes in the mean wind field. Spectral analyses of

tropical data also suggest a variability in wave structure. Wallace and Chang (1969) found that the easterly wave-type disturbances had very little vertical tilt while Yanai et al. (1968) obtained an appreciable eastward tilt with height.

It was pointed out in the introduction that, while mature tropical wave disturbances may be driven by latent heat of condensation, they may originate from barotropic instability in the easterlies (Bates 1970). If these disturbances arise in this way, they should retain certain features (wavelength, latitudinal structure, etc.) of the barotropically unstable modes. Thus the wave structures obtained in this paper may be relevant to tropical wave disturbances that are driven by latent heat of condensation.

The studies of this paper should be continued with a primitive equation model having adequate vertical resolution. Parameterized latent heat of condensation as well as a proper treatment of the surface friction should be included.

ACKNOWLEDGMENTS

The authors thank Profs. R.L. Elsberry, G.J. Haltiner, and J.R. Holton for reading the manuscript and for making useful comments. The manuscript was carefully typed by Mrs. Joann Madler and Mrs. Sheila San Chirico.

This research was partially supported by the Navy Weather Research Facility. The numerical computations were performed by the W.R. Church Computer Center at the Naval Postgraduate School and by the University of Utah Computer Center.

REFERENCES

- Bates, J. R., "Dynamics of Disturbances on the Intertropical Convergence Zone," *Quarterly Journal of the Royal Meteorological Society*, Vol. 96, No. 410, London, England, Oct. 1970, pp. 677-701.
- Betchov, Robert, and Criminale, William, *Stability of Parallel Flows*, Academic Press, New York, N.Y., 1967, 330 pp.
- Case, K. M., "Stability of Inviscid Plane Couette Flow," *Physics of Fluids*, Vol. 3, No. 2, Mar.-Apr. 1960, pp. 143-157.
- Chang, Chih-Pei, Morris, V. F., and Wallace, John M., "A Statistical Study of Easterly Waves in the Western Pacific: July-December 1964," *Journal of the Atmospheric Sciences*, Vol. 27, No. 2, Mar. 1970, pp. 195-201.
- Charney, Jule G., "A Note on Large-Scale Motions in the Tropics," *Journal of the Atmospheric Sciences*, Vol. 20, No. 6, Nov. 1963, pp. 607-609.
- Charney, Jule G., "A Further Note on Large-Scale Motions in the Tropics," *Journal of the Atmospheric Sciences*, Vol. 26, No. 1, Jan. 1969, pp. 182-185.
- Charney, Jule G., and Eliassen, Arnt, "A Numerical Method for Predicting the Perturbations in the Middle-Latitude Westerlies," *Tellus*, Vol. 1, No. 2, Stockholm, Sweden, May 1949, pp. 38-54.
- Charney, Jule G., and Eliassen, Arnt, "On the Growth of the Hurricane Depression," *Journal of the Atmospheric Sciences*, Vol. 21, No. 1, Jan. 1964, pp. 68-75.
- Garcia, K. V., "Barotropic Waves in Straight Parallel Flow With Curved Velocity Profile," *Tellus*, Vol. 8, No. 1, Stockholm, Sweden, Feb. 1956, pp. 82-93.
- Greenspan, H.P., *The Theory of Rotating Fluids*, Cambridge University Press, England, 1968, 327 pp. (see p. 7).
- Holton, James R., "A Diagnostic Model for Equatorial Wave Disturbances," *Journal of the Atmospheric Sciences*, Vol. 28, No. 1, Jan. 1971, pp. 55-64.
- Holton, James R., Wallace, John M., and Young, J. A., "Boundary Layer Dynamics and the ITCZ," *Journal of the Atmospheric Sciences*, Vol. 28, No. 2, Mar. 1971, pp. 275-280.

- Jacobs, Stanley J., and Wiin-Nielsen, Aksel, "On the Stability of a Barotropic Basic Flow in a Stratified Atmosphere," *Journal of the Atmospheric Sciences*, Vol. 23, No. 6, Nov. 1966, pp. 682-687.
- Kuo, Hsiao-Lan, "Dynamic Instability of Two-Dimensional Nondivergent Flow in a Barotropic Atmosphere," *Journal of Meteorology*, Vol. 6, No. 2, Apr. 1949, pp. 105-122.
- Kuo, Hsiao-Lan, "On Formation and Intensification of Tropical Cyclones Through Latent Heat Release by Cumulus Convection," *Journal of the Atmospheric Sciences*, Vol. 22, No. 1, Jan. 1965, pp. 40-63.
- La Seur, Noel E., "Synoptic Models in the Tropics: A Survey Paper," *Proceedings of the Symposium on Tropical Meteorology, Rotorua, New Zealand, November 5-13, 1963*, New Zealand Meteorological Service, Wellington, 1964, pp. 319-328.
- Lipps, Frank B., "The Barotropic Stability of the Mean Winds in the Atmosphere," *Journal of Fluid Mechanics*, Vol. 12, No. 3, London, England, Mar. 1962, pp. 397-407.
- Lipps, Frank B., "Barotropic Stability and Tropical Disturbances," *Monthly Weather Review*, Vol. 98, No. 2, Feb. 1970, pp. 122-131.
- Manabe, Syukuro, Holloway, J. Leith, Jr., and Stone, Hugh, "Tropical Circulation in a Time-Integration of a Global Model of the Atmosphere," *Journal of the Atmospheric Sciences*, Vol. 27, No. 4, July 1970, pp. 580-613.
- Matsuno, Taroh, "Quasi-Geostrophic Motions in the Equatorial Area," *Journal of the Meteorological Society of Japan*, Ser. 2, Vol. 44, No. 1, Tokyo, Feb. 1966, pp. 25-43.
- Merritt, Earl S., "Easterly Waves and Perturbations, a Reappraisal," *Journal of Applied Meteorology*, Vol. 3, No. 4, Aug. 1964, pp. 367-382.
- Nitta, Tsuyoshi, "A Study of the Generation and Conversion of Eddy Available Potential Energy in the Tropics," *Journal of the Meteorological Society of Japan*, Ser. 2, Vol. 48, No. 6, Tokyo, Dec. 1970, pp. 127-130.
- Nitta, Tsuyoshi, and Yanai, Michio, "A Note on the Barotropic Instability of the Tropical Easterly Current," *Journal of the Meteorological Society of Japan*, Ser. 2, Vol. 47, No. 2, Tokyo, Apr. 1969, pp. 127-130.
- Ooyama, Katsuyuki, "Numerical Simulation of the Life Cycle of Tropical Cyclones," *Journal of the Atmospheric Sciences*, Vol. 26, No. 1, Jan. 1969, pp. 3-40.
- Palmer, Clarence Edgar, "Tropical Meteorology," *Compendium of Meteorology*, American Meteorological Society, Boston, Mass., 1951, 1334 pp. (see pp. 859-880).
- Pedlosky, Joseph, "An Initial Value Problem in the Theory of Barotropic Instability," *Tellus*, Vol. 16, No. 1, Stockholm, Sweden, Feb. 1964, pp. 12-17.
- Richtmyer, Robert D., *Difference Methods for Initial Value Problems*, Interscience Publishers, Inc., New York, N.Y., 1957, 238 pp.
- Riehl, Herbert, "Waves in the Easterlies," *Tropical Meteorology*, McGraw-Hill Book Co., Inc., New York, N.Y., 1954, 392 pp. (see pp. 210-234).
- Sadler, J. S., "TIROS Observations of the Summer Circulation and Weather Patterns of the Eastern North Pacific," *Proceedings of the Symposium on Tropical Meteorology, Rotorua, New Zealand, November 5-13, 1963*, New Zealand Meteorological Service, Wellington, 1964, pp. 553-571.
- Starr, Victor P., and Wallace, John M., "Mechanics of Eddy Processes in the Tropical Troposphere," *Pure and Applied Geophysics*, Vol. 58, No. 2, Basel, Switzerland, 1964, pp. 138-144.
- Wallace, John M., and Chang, Chih-Pei, "Spectrum Analysis of Large-Scale Wave Disturbances in the Tropical Lower Troposphere," *Journal of the Atmospheric Sciences*, Vol. 26, No. 5, Pt. 2, Sept. 1969, pp. 1010-1025.
- Yamasaki, Masanori, "Large-Scale Disturbances in the Conditionally Unstable Atmosphere in Low Latitudes," *Papers in Meteorology and Geophysics*, Vol. 20, No. 4, Tokyo, Japan, Dec. 1969, pp. 289-336.
- Yanai, Michio, "Dynamical Aspects of Typhoon Formation," *Journal of the Meteorological Society of Japan*, Ser. 2, Vol. 39, No. 5, Tokyo, Oct. 1961, pp. 282-309.
- Yanai, Michio, Maruyama, T., Nitta, T., and Hayashi, Y., "Power Spectra of Large-Scale Disturbances Over the Tropical Pacific," *Journal of the Meteorological Society of Japan*, Ser. 2, Vol. 46, No. 4, Tokyo, Aug. 1968, pp. 308-323.
- Yanai, Michio, and Nitta, Tsuyoshi, "Computation of Vertical Motion and Vorticity Budget in a Caribbean Easterly Wave," *Journal of the Meteorological Society of Japan*, Ser. 2, Vol. 45, No. 6, Dec. 1967, pp. 444-466.
- Yanai, Michio, and Nitta, Tsuyoshi, "Finite Difference Approximations for the Barotropic Instability Problem," *Journal of the Meteorological Society of Japan*, Ser. 2, Vol. 46, No. 5, Tokyo, Oct. 1968, pp. 389-403.
- Zipser, Edward J., "The Role of Organized Unsaturated Convective Downdrafts in the Structure and Rapid Decay of an Equatorial Disturbance," *Journal of Applied Meteorology*, Vol. 8, No. 5, Oct. 1969, pp. 799-814.

[Received June 29, 1970; revised June 9, 1971]